

A COMPARISON OF SURFACE PROPERTIES OF METALLIC THIN FILM PHOTOCATHODES

S. Mistry, M. Cropper, Department of Physics, Loughborough University, Loughborough, Leicestershire, LE11 3TU, UK

R. Valizadeh, L.B. Jones, K.J. Middleman, A.N. Hannah, B.L. Milityn and T.C.Q. Noakes, STFC ASTeC, Daresbury, Warrington, Cheshire, WA4 4AD, UK

Abstract

In this work the preparation of metal photocathodes by physical vapour deposition magnetron sputtering has been employed to deposit metallic thin films onto Cu, Mo and Si substrates. The use of metallic cathodes offers several advantages: (i) metal photocathodes present a fast response time and a relative insensitivity to the vacuum environment (ii) metallic thin films when prepared and transferred in vacuum can offer smoother and cleaner emitting surfaces. The photocathodes developed here will ultimately be used in S-band Normal Conducting RF (NCRF) guns such as that used in VELA (Versatile Electron Linear Accelerator) and the proposed CLARA (Compact Linear Accelerator for Research and Applications) Free Electron Laser test facility. The samples grown on Si substrates were used to investigate the morphology and thickness of the film. The samples grown onto Cu and Mo substrates were analysed and tested as photocathodes in a surface characterisation chamber, where X-Ray Photoelectron spectroscopy (XPS) was employed to determine surface chemistry and Ultraviolet Photoelectron spectroscopy (UPS) technique was used to determine work function. QE measurements were enabled using a 266 nm UV laser.

INTRODUCTION

Linac driven FELs have stringent requirements particularly with respect to the photocathode used in the photoinjector. The principal photocathode properties are Quantum Efficiency (QE), emitted electron transverse and longitudinal energy spread, response time and life time. Depending on the characteristics required from the electron bunch, a suitable cathode material is chosen. For example, metals exhibit a fast (femtosecond) response time which enables the production of short electron pulses. The VELA photo-injector at Daresbury Laboratory, uses a copper disk photocathode for this reason [1]. Though notoriously poor with regards QE, copper has typically been the choice photocathode material for NCRF guns because it is easy to handle and is relatively insensitive to the vacuum environment [2]. Using different materials with higher quantum yield in RF-guns is limited because of the issue of RF breakdown in the joint between the two metals [3]. The use of thin films deposited onto a suitable substrate could evade these problems, thus opening up the possibility of

implementing an alternative metal to copper that exhibits better photocathode performance.

Much research has been carried out investigating different methods of developing thin film photocathodes so as to increase the adhesion of the thin film to the substrate, such as pulsed laser deposition, evaporation, arc deposition and sputtering. In this study Physical Vapour Deposition (PVD) magnetron sputtering has been employed to adhere Pb, Zr and Cu thin films onto Cu, Mo, Si substrates. Molybdenum is the choice substrate material for the CLARA [4] photocathode and copper has been selected as the baseline photocathode material. The films deposited onto silicon substrates were used to characterise the morphology of the film.

EXPERIMENTAL PROCEDURE

Cu, Pb and Zr thin films were produced by DC magnetron sputtering onto Cu, Mo and Si substrates. The substrates were cleaned and degreased in ultrasonic baths of acetone and then washed in deionised water.

Kr sputter gas was used at approximately $5 \cdot 10^{-2}$ mbar at ambient temperature for each deposition using pulsed DC power supply. The parameters are listed below in Table 1. As a precautionary measure, Pb was deposited at a lower power due to its lower melting temperature.

Table 1: Deposition Parameters

Metal	DC Power (W)	Pressure (mbar)	Time (hrs)
Cu	300	$5.4 \cdot 10^{-2}$	1
Pb	100	$4.3 \cdot 10^{-2}$	3
Zr	300	$8.5 \cdot 10^{-2}$	1

Each thin film was subsequently taken out of the chamber and stored at atmosphere for a short period of time prior to loading into the SAPI (Surface Analysis Preparation and Installation) [5] system for analysis.

The samples were characterised in the SAPI analysis chamber under UHV conditions and ambient temperature.

The QE of the photoemission was measured using a custom-made apparatus. A schematic of the experimental arrangement for QE measurements is shown in Fig. 1. Thin film samples were biased at -18 V with a battery box that was connected as shown below between the electrical feedthrough and a Keithley type 480 picoammeter.

To achieve photoemission a compact UV laser source has been implemented onto the SAPI system. The laser is a commercial system (Crylas FQSS 266-Q4). A diode generates light at 1064 nm, is then frequency-doubled to generate 532 nm, and then doubled again to generate a 266 nm UV beam. This has a line width < 0.1 nm, with a TEM₀₀ spatial mode. The laser beam was pulsed using a passive Q-switch, and it delivers a 1 kHz repetition of approximately 1 ns pulses with an individual pulse energy of more than 12 mJ, focused to a spot size of *ca* 3 mm FWHM. The average UV power was measured to be around 16.3 mW using a photodiode. Unfortunately, because the diode normally used to calibrate the UV flux in-situ was not functional, care must be taken when comparing these results with work function measurements presented in previous papers [6]. Nonetheless these measurements should be indicative of the relative changes in work function (ϕ) between experiments presented here.

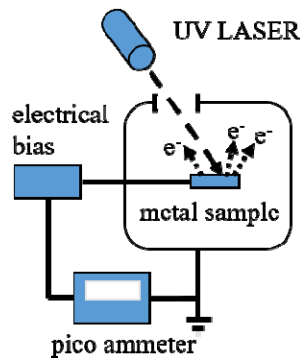


Figure 1: Schematic diagram of the total-yield QE measurement circuit.

The cathode chemical composition was determined using XPS at 1486.6eV (Al K α) photon energy and with a resolution of 1.1 eV. Thermo Scientific Advantage software was used to analyse the spectra obtained. A standard Shirley background was used for all spectral regions.

UPS was employed to obtain the full width of the photoemission spectrum, from the fermi edge to the secondary electron cut-off, with the samples biased at 9 V. Using equation 1, a value for ϕ can be calculated.

$$\phi = h\nu - W \quad (1)$$

where ϕ is the work function, h is planck's constant, ν is the frequency and W is the full width.

The 1 UV radiation (21.2 eV), generated from a gas discharge lamp, was irradiated on the sample surface and the emitted electrons energy analysed with a hemispherical analyser.

Due to atmospheric exposure between deposition and analysis, the sample surfaces were oxidised. Therefore after analysis "as-received," the samples were Ar⁺ sputter cleaned (45 minute at 2 keV and approximately 2.5 μ A) to remove surface contaminants.

RESULTS AND DISCUSSION

Copper Thin Films

Quantification of the elemental composition was obtained from XPS survey spectra. For both the "as received" Cu films the surface chemical state consisted of CuO. Upon sputter cleaning, the percentage of O 1s is reduced to undetectable levels. Details of the particular chemical state of the surface layers can be extracted from the Cu LMM region spectra shown in Fig. 2. The "as received" Cu LMM region spectra is characteristic of CuO whereas the Ar⁺ sputtered spectra describes Cu metal [7].

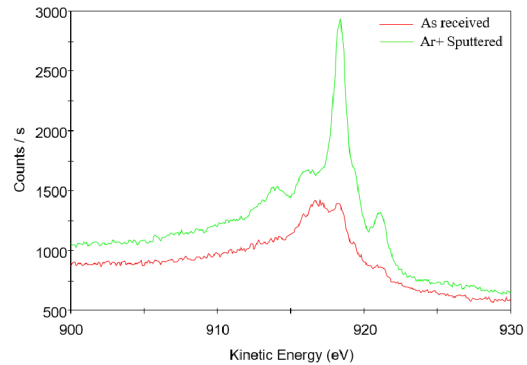


Figure 2: XPS Cu LMM region spectra for Cu on Cu thin film.

The effects of oxidation on the emissive properties of the Cu thin films is described below. Table 2 summarises the measurements of QE and ϕ "as received" and after sputtering.

Table 2: Summary of ϕ and QE Data for Cu Thin Films

	As received		Ar ⁺ Sputtered	
	ϕ (eV)	QE	ϕ (eV)	QE
Cu on Cu	5.37	$2.5 \cdot 10^{-6}$	4.47	$6.5 \cdot 10^{-6}$
Cu on Mo	5.39	$2.4 \cdot 10^{-6}$	4.45	$7.4 \cdot 10^{-6}$

The ϕ values for thin films deposited on Cu and Mo are 5.37 eV and 5.39 eV respectively. For a clean polycrystalline Cu surface, the work function is expected to be approximately 4.65 eV [8], and so an oxidised surface will typically yield a higher value. After sputter cleaning the samples, the ϕ values reduce by almost 1 eV. The reduction of ϕ correlates with an increase in the QE value. This is of course to be expected; the lower the ϕ the less energy is required for photoelectrons to overcome the potential barrier and escape to vacuum.

Lead Thin Films

Table 3: Quantitative XPS Data for Pb Thin Films

	As received		Ar ⁺ Sputtered	
	O1s	Pb 4f	O1s	Pb 4f
Pb on Cu	36.91	63.09	0	100
Pb on Mo	57.99	42.01	0	100

Table 3 shows a summary of the elemental composition for Pb thin films as extracted from XPS survey spectra. For the Pb on Cu sample, the surface is significantly less oxidised compared with the Pb on Mo sample. This is because the film deposited on Mo was stored at atmosphere for 24 hours prior to analysis, whereas the Pb on Cu sample was analysed straight away. Fig. 3 shows the Pb 4f region spectra for the Pb on Cu sample “as received” and after sputter treatment. From the “as received” spectra we can see that the Pb 4f_{7/2} peak can be resolved into two peaks; one at 137.2 eV indicative of Pb metal and the other at 138.1 eV which highlights lead oxide, PbO₂. The effect of sputter cleaning is to remove the surface oxide layers; this is evidenced by the shift in the Pb 4f peaks and change in shape. A similar change was observed for the Pb on Mo sample.

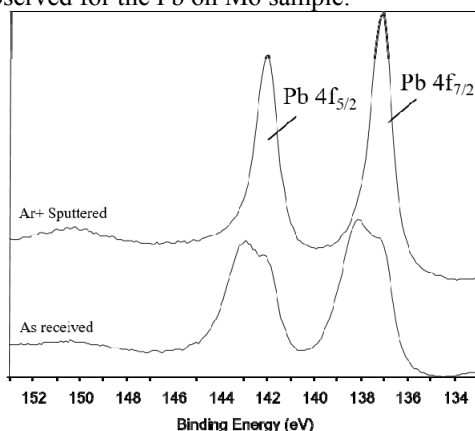


Figure 3: XPS Pb 4f region spectra for Pb on Cu thin film.

The literature values for the ϕ of Pb range between 4.25-4.14 eV [8, 9]. The partially oxidised Pb on Cu sample was measured to have a ϕ of 4.24 eV, and the clean surface had a reduced ϕ of 4.08 eV (see Table 4). The QE value increases by a factor of two upon Ar⁺ sputtering.

In the case of the Pb on Mo film, the ϕ value “as received” is more than 1 eV higher than the ϕ value for the Pb on Cu film. This can perhaps be attributed to the higher content of oxygen on the sample surface (see Table 3).

Table 4: Summary of ϕ and QE Data for Pb Thin Films

	As received		Ar ⁺ Sputtered	
	ϕ (eV)	QE	ϕ (eV)	QE
Pb on Cu	4.24	$1.7 \cdot 10^{-5}$	4.08	$2.6 \cdot 10^{-5}$
Pb on Mo	5.21	$1.2 \cdot 10^{-5}$	4.06	$2.8 \cdot 10^{-5}$

Zirconium Thin Films

As with the Cu and Pb films, oxidised surfaces layers were removed by Ar⁺ sputtering. This is evidenced by the survey spectra for Zr film on Cu shown in Fig. 4. The effect of this on the ϕ and the photo-emissivity of the Zr films is summarised in Table 5.

The QE values are comparable for the both the Zr film deposited on Cu and Mo substrates. As expected, the reduction of surface oxide correlates with a reduction in work function leading to a higher QE.

Particularly in the case of the Zr films “as received,” defining a sharp fermi-edge from which to determine the work function proved to be difficult. Therefore the ϕ values calculated for oxidised Zr films have a larger error bar.

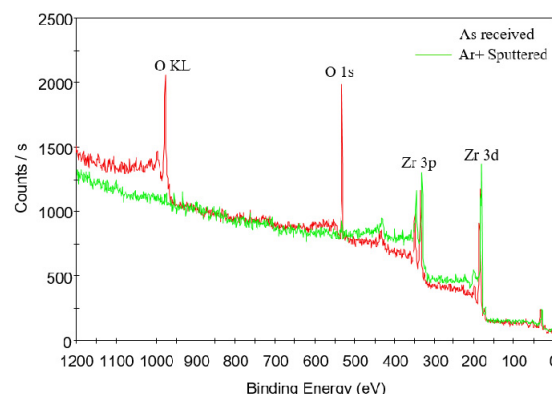


Figure 4: XPS Survey spectra for Zr on Cu thin film.

Table 5: Summary of ϕ and QE Data for Zr Thin Films

	As received		Ar ⁺ Sputtered	
	ϕ (eV)	QE	ϕ (eV)	QE
Zr on Cu	*6.12	$3.8 \cdot 10^{-6}$	3.67	$1.5 \cdot 10^{-5}$
Zr on Mo	*5.89	$4.7 \cdot 10^{-6}$	3.60	$1.5 \cdot 10^{-5}$

The ϕ values after sputtering the Zr films are lower than literature values by approximately 0.3-0.4 eV [8]. If the ϕ of the sputtered surface was indeed as low as measured, then a significantly higher than measured QE value was to be expected. This could perhaps be explained by the damaging effects on the metal surfaces caused by Ar⁺ sputtering. However, further investigations are required to bring greater clarity to this phenomena.

CONCLUSION

The photocathode and surface properties of the three metals investigated in this study are independent of the substrate material used. Despite exposure to atmosphere, clean sample surfaces were achievable by employing Ar⁺ bombardment. Of the three materials investigated in this study, Pb thin film exhibits the highest QE of $2.6 \cdot 10^{-5}$ at 266 nm. Further work will include experiments with Mg, Nb and Ti thin films.

ACKNOWLEDGMENT

The work is part of EuCARD-2, partly funded by the European Commission, GA 312453.

REFERENCES

- [1] P. McIntosh et al, Proc of IPAC'13, Shanghai, China, pp. 3708-3710, paper THPWA036.
- [2] A. Lorusso et al, Phys. Rev S. T.- A. & B. 14.9 (2011).

- [3] A. Perrone et al. N. I. M. Phys Res. A: 554.1 (2005).
- [4] J.A. Clarke, et al. J. Instrum. 9.05 (2014): T05001.
- [5] T.C.Q Noakes EuCARD2 MS575 EDMS: 1325281, 2014.
- [6] S. Mistry et al. Proc of IPAC'15, Richmond, USA, pp. 1759-1761, paper TUPJE058.
- [7] S. Poulston , et al, Surf. Interface Anal. Vol. 24, 811-82, 1996.
- [8] H.B. Michaelson, J. Appl. Phys. 48, 4729, 1977.
- [9] P. A. Anderson et al, Phys. Rev., Vol. 102, 1956.